The 5th International Power Engineering and Optimization Conference (PEOCO2011), Shah Alam, Selangor, Malaysia : 6-7 June 2011

Investigation of Induction Motor Drive Behavior in Low-cost Fault Tolerant Control for Electric Vehicles

Hamed Shahsavari Alavije[1], Mahdi Akhbari [2]
[1], [2] Electrical& Electronic Eng.Dept. Shahed University. Tehran, Iran.
[1] Shahsavari@ieee.org, [2] akhbari@shahed.ac.ir

Abstract: ***In this paper, the induction motor drive behavior in a low-cost fault tolerant control system for electric vehicles is investigated. The presented control strategy focuses on the faults of inverter power switches (i.e. short-circuit and open circuit of the inverter legs). The induction motor drive system is based on a voltage source inverter (VSI) controlled with space vector modulation (SVM) algorithm. The presented control system is able to adaptively change-over to different control algorithms when the faults are occurred; also it creates the smooth transitions of the motor current, torque and speed when changing over between the switching algorithms. A 15kW induction motor is used for simulations. The results of the simulations: stator current, electromagnetic torque and speed regulation behaviors demonstrate the performance and validity of the presented fault-tolerant control for induction motor drive fault mitigation.***

Index Terms: **Electrical vehicles, fault tolerant, induction motor, SVM, four-switch inverter.**

1. Introduction

One of the important issues in electrical vehicle (EV) traction application is electric-propulsion. Electric-propulsion control system has some major requirements that are summarized as follows [1], [2]:

- High instant power and high power density;
- High torque at low speeds for starting and climbing, as well as high power at high speed for cruising;
- Very wide speed range including constant-torque and constant-power regions;
- Fast torque response;
- High efficiency over wide speed and torque ranges;
- High efficiency for regenerative braking;
- High reliability and robustness for various vehicle-operating conditions; and
- Reasonable cost.

Proper operation of this control system depends on the reliable performance of electric-motor, three-phase inverter and control and instrumentation circuitry. Each of these sections may have a fault in their operations that are summarized as follows [3]:

Electric-motor faults include:

- Single phase failure
- Multi-phase failure
- Eccentricity
- Demagnetization

Three-phase inverter faults include:

- Component failure
- Single leg failure
- Multiple leg failure
- Failure in gate drivers
- Failure in interface

And control and instrumentation circuitry faults include:

- Failure of position encoder
- Failure of sensorless control
- Failure of current sensor
- Failure of filter and signal conditioning circuit

Several failures can affect electrical-motor drives, and many different treatment methods have been proposed [4]-[8]. Therefore, redundant or conservative design has been used to robust continuity operation in a reasonable state when the faults are occurred. Some of these designs may have short torque transients and even reduced drive performance after a fault, on the condition that the drive still goes running. This is especially important in EV electrical-motor drives that should have high reliability and robustness for various vehicle-operation conditions. This paper describes a low-cost fault tolerant control system in induction motor drive for EV. The presented control strategy focuses on the faults of inverter power switch (i.e. short-circuit and open circuit of the inverter legs). Many different control strategies and circuit topologies have been proposed to provide fault tolerant capabilities under the conditions [6],[8]-[13]. The presented control strategy runs closed-loop conventional SVM algorithm for six-switch inverter topology with extra switches that will be used by fault tolerant control (Figure 1). When one of the inverter legs is lost (the short-circuit leg is disconnected by fuse, also it will be such as an open circuit), it change-overs to a closed-loop modified SVM algorithm for four-switch inverter topology by one of the extra switches (Figure 2), and it connects the stator winding that lost the third leg of six-switch inverter, to the middle point of a capacitor bank. In the following sections the equations of conventional SVM algorithm for six-switch inverter topology and the

978-1-4577-0354-6/11/$26.00 ©2011 IEEE

modified SVM algorithm for four-switch inverter topology is derived. Then the simulation procedures and results: stator current, electromagnetic torque and speed regulation behaviors are shown.

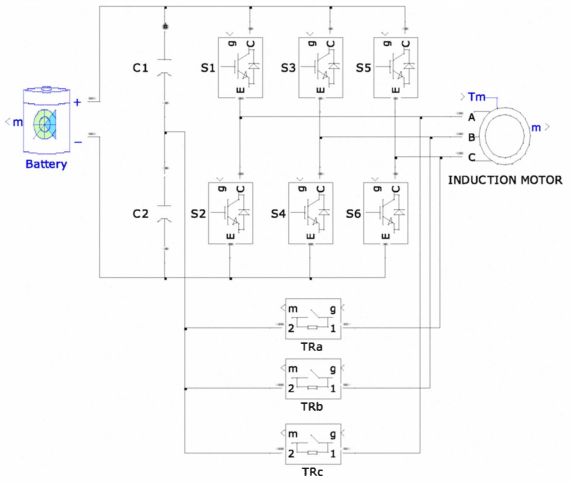

Figure 1 Six-switch inverter topology with extra switches

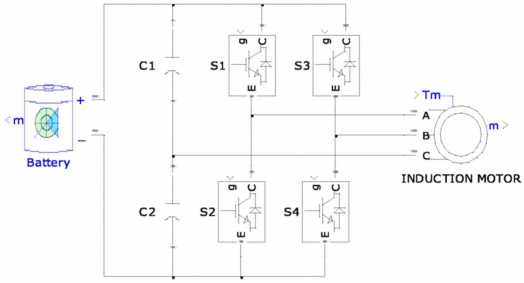

Figure 2 Four-switch inverter topology

2. Space Vector Modulation

The switching status of circuit in Figure 1 and Figure 2 is represented by the binary variables S_1 to S_6 and S_1 to S_4 respectively, which values of '1' and '0' indicate closed and open switch respectively. In addition, the switches of each leg are controlled complementary (i.e. $S_2 = 1 - S_1$). In the following phase voltages, vector voltages and switching time calculation are derived (Z is negative pole of battery and N is neutral point of motor).

2.1 Six-Switch Inverter Algorithm

Pole voltages of motor in Figure 1are determined by the switching status can be obtained as:

$$V_{AZ} = S_1 \cdot V_{bat} \quad (1)$$

$$V_{BZ} = S_3 \cdot V_{bat} \quad (2)$$

$$V_{CZ} = S_5 \cdot V_{bat} \quad (3)$$

And:

$$V_{NZ} = 1/3\,(V_{AZ} + V_{BZ} + V_{CZ}) \quad (4)$$

Therefore, phase voltages can be written as:

$$V_{AN} = V_{AZ} - V_{NZ} \quad (5)$$

$$V_{BN} = V_{BZ} - V_{NZ} \quad (6)$$

$$V_{CN} = V_{CZ} - V_{NZ} \quad (7)$$

Combinations of switching S_1 to S_6 produce six different space vector voltages that are shown in Figure 3 and Table 1.Vectorial voltages are done by using equation 8.

$$\begin{bmatrix} x_\alpha \\ x_\beta \end{bmatrix} = \frac{2}{3}\begin{bmatrix} 1 & -\frac{1}{2} & -\frac{1}{2} \\ 0 & \frac{\sqrt{3}}{2} & -\frac{\sqrt{3}}{2} \end{bmatrix}\begin{bmatrix} x_a \\ x_b \\ x_c \end{bmatrix} \quad (8)$$

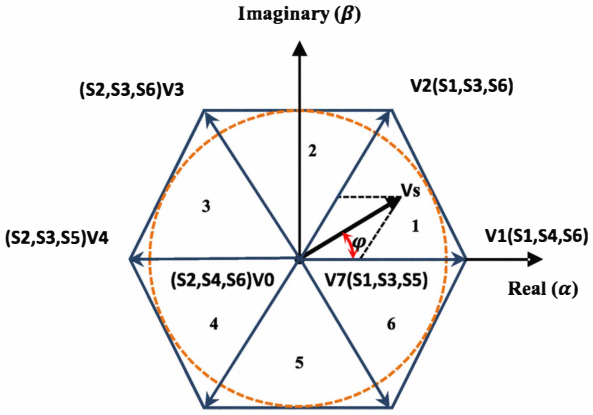

Figure 3 Space vector voltages of different switching status in six-switch inverter

Table 1.Vectorial voltages in six-switch inverter

Vector	On Switch	V_{AZ}	V_{BZ}	V_{CZ}	$\vec{v}_{\alpha\beta}$
$\vec{V}_0$	$S_2S_4S_6$	0	0	0	$\vec{0}$
$\vec{V}_1$	$S_1S_4S_6$	V_{bat}	0	0	$\frac{2V_{bat}}{3}e^{j0}$
$\vec{V}_2$	$S_1S_3S_6$	V_{bat}	V_{bat}	0	$\frac{2V_{bat}}{3}e^{j\frac{\pi}{3}}$
$\vec{V}_3$	$S_2S_3S_6$	0	V_{bat}	0	$\frac{2V_{bat}}{3}e^{j\frac{2\pi}{3}}$
$\vec{V}_4$	$S_2S_3S_5$	0	V_{bat}	V_{bat}	$\frac{2V_{bat}}{3}e^{j\pi}$
$\vec{V}_5$	$S_2S_4S_5$	0	0	V_{bat}	$\frac{2V_{bat}}{3}e^{j\frac{-2\pi}{3}}$
$\vec{V}_6$	$S_1S_4S_5$	$\frac{2V_{bat}}{3}$	0	V_{bat}	$\frac{2V_{bat}}{3}e^{j\frac{-\pi}{3}}$
$\vec{V}_7$	$S_1S_3S_5$	V_{bat}	V_{bat}	V_{bat}	$\vec{0}$

Each desired position on circular for the vector voltage V_S in Figure 3 can be achieved by a time average relationship between two neighbouring active vectors (t_a&t_b). Zero state vectors (t_0) are used to fill up the gap to a constant sampling interval T_S. To calculate t_a&t_b &t_0, decomposition V_S along Real and Imaginary axes in Figure 3:

$$\vec{V}_S T_S = \vec{V}_1 t_a + \vec{V}_2 t_b + \vec{V}_0 \frac{t_0}{2} + \vec{V}_7 \frac{t_0}{2} \quad (9)$$

$$T_s = t_a + t_b + t_0 \quad (10)$$

$$\text{Real: } V_S \cdot \cos\varphi \cdot T_S = \frac{2V_{bat}}{3} \cdot 1 \cdot t_a + \frac{2V_{bat}}{3} \cdot \frac{1}{2} \cdot t_b \quad (11)$$

$$\text{Imag:} V_S \cdot \sin\varphi \cdot T_S = \frac{2V_{bat}}{3} \cdot 0 \cdot t_a + \frac{2V_{bat}}{3} \cdot \frac{\sqrt{3}}{2} \cdot t_b \quad (12)$$

With the solution:

$$t_a = \frac{3 \cdot T_S}{2 \cdot V_{bat}} \left(v_x - \frac{1}{\sqrt{3}} \cdot v_y \right) \quad (13)$$

$$t_b = \frac{\sqrt{3} \cdot T_S}{V_{bat}} (v_y) \quad (14)$$

$$t_0 = T_S - t_a - t_b \quad (15)$$

That $v_x = V_S \cdot \cos\varphi$, $v_y = V_S \cdot \sin\varphi$.

t_a&t_b in all sectors are shown in Table 2:

Table 2. Switching time in each sector

Sec1	$t_a = \frac{3 \cdot T_S}{2 \cdot V_{bat}} \left(v_x - \frac{1}{\sqrt{3}} \cdot v_y \right)$	$t_b = \frac{\sqrt{3} \cdot T_S}{V_{bat}} (v_y)$
Sec2	$t_a = \frac{3 \cdot T_S}{2 \cdot V_{bat}} \left(v_x + \frac{1}{\sqrt{3}} \cdot v_y \right)$	$t_b = \frac{3 \cdot T_S}{2 \cdot V_{bat}} \left(-v_x + \frac{1}{\sqrt{3}} \cdot v_y \right)$
Sec3	$t_a = \frac{\sqrt{3} \cdot T_S}{V_{bat}} (v_y)$	$t_b = \frac{3 \cdot T_S}{2 \cdot V_{bat}} \left(-v_x - \frac{1}{\sqrt{3}} \cdot v_y \right)$
Sec4	$t_a = \frac{3 \cdot T_S}{2 \cdot V_{bat}} \left(-v_x + \frac{1}{\sqrt{3}} \cdot v_y \right)$	$t_b = \frac{-\sqrt{3} \cdot T_S}{V_{bat}} (v_y)$
Sec5	$t_a = \frac{3 \cdot T_S}{2 \cdot V_{bat}} \left(-v_x - \frac{1}{\sqrt{3}} \cdot v_y \right)$	$t_b = \frac{3 \cdot T_S}{2 \cdot V_{bat}} \left(v_x - \frac{1}{\sqrt{3}} \cdot v_y \right)$
Sec6	$t_a = \frac{-\sqrt{3} \cdot T_S}{V_{bat}} (v_y)$	$t_b = \frac{3 \cdot T_S}{2 \cdot V_{bat}} \left(v_x + \frac{1}{\sqrt{3}} \cdot v_y \right)$

2.2 Four-Switch Inverter Algorithm

Pole voltages of motor in Figure 2 are determined by the switching status can be obtained as:

$$V_{AZ} = S_1 \cdot V_{bat} \quad (16)$$

$$V_{BZ} = S_3 \cdot V_{bat} \quad (17)$$

$$V_{CZ} = V_{bat}/2 \quad (18)$$

And:

$$V_{NZ} = 1/3 \, (V_{AZ} + V_{BZ} + V_{CZ}) \quad (19)$$

Therefore, phase voltages can be written as:

$$V_{AN} = V_{AZ} - V_{NZ} \quad (20)$$

$$V_{BN} = V_{BZ} - V_{NZ} \quad (21)$$

$$V_{CN} = V_{CZ} - V_{NZ} \quad (22)$$

Like six-switch inverter, combinations of switching S_1 to S_4 produce four different space vector voltages that are shown in Figure 4 and Table 3.Vector voltages are done by using equation 8.

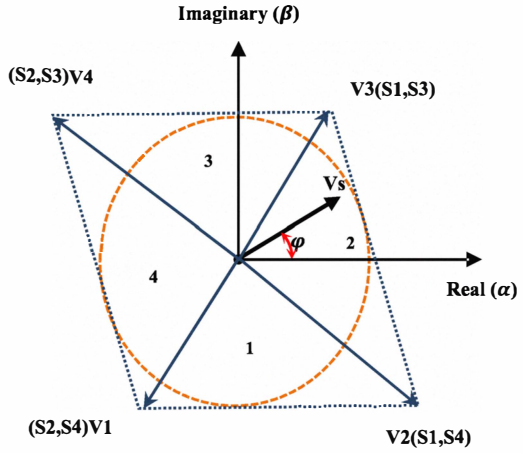

Figure 4.Space vector voltages of different switching status in four-switch inverter [8]

Table 3. Vector voltages in four-switch inverter

Vector	On Switch	V_{AZ}	V_{BZ}	V_{CZ}	$\vec{v}_{\alpha\beta}$
$\vec{V}_1$	S_2S_4	0	0	$V_{bat}/2$	$\frac{V_{bat}}{3} \cdot e^{-j\frac{2\pi}{3}}$
$\vec{V}_2$	S_1S_4	V_{bat}	0	$V_{bat}/2$	$\frac{\sqrt{3}V_{bat}}{3} \cdot e^{-j\frac{\pi}{6}}$
$\vec{V}_3$	S_1S_3	V_{bat}	V_{bat}	$V_{bat}/2$	$\frac{V_{bat}}{3} \cdot e^{j\frac{\pi}{3}}$
$\vec{V}_4$	S_2S_3	0	V_{bat}	$V_{bat}/2$	$\frac{\sqrt{3}V_{bat}}{3} \cdot e^{j\frac{5\pi}{6}}$

As it can be seen in Table 3, four-switch inverter has no zero vectors. This means that in order to fill up the gap to a constant sampling interval T_S, modified SVM algorithm should be developed based on the remaining active vectors (Figure 4).The switching time equation is:

$$\vec{V}_S T_S = \vec{V}_1 t_1 + \vec{V}_2 t_2 + \vec{V}_3 t_3 + \vec{V}_4 t_4 \quad (23)$$

The opposite vectors V_1&V_3 or V_2&V_4 can be used to make zero vector to fill up the gap. Only three of four vectors are required to accurately define the magnitude and the phase of $\vec{V}_S$ during the switch period T_S. There are two possibilities to select three vectors. It is better to select two short and one leg vectors instead of two long and one short; because the long vectors make larger voltage drop on inductive loads and larger ripple. So on that, there are two groups of three vectors; one group include the long vector $\vec{V}_2$ and the other group include the long vector $\vec{V}_4$. So to derive SVM timings there are two groups of adjacent sectors in vector space.

Sector 1 and 2 ($-\frac{2\pi}{3} < \varphi < \frac{\pi}{3}$)

The switching time equation is:

$$\vec{V}_S T_S = \vec{V}_1 t_1 + \vec{V}_2 t_2 + \vec{V}_3 t_3 \quad (24)$$

The vector decomposition of the above equation along Real and Imaginary axes in Figure 4:

$$T_S = t_1 + t_2 + t_3 \quad (25)$$

$$Real: \quad V_S T_S \cos\varphi = -V_1 t_1 \cos\frac{\pi}{3} + V_2 t_2 \cos\frac{\pi}{6} + V_3 t_3 \cos\frac{\pi}{3} \quad (26)$$

$$Imag: \quad V_S T_S \sin\varphi = -V_1 t_1 \sin\frac{\pi}{3} - V_2 t_2 \sin\frac{\pi}{6} + V_3 t_3 \sin\frac{\pi}{3} \quad (27)$$

With the solution:

$$t_2 = \frac{\sqrt{2} V_S T_S}{V_{bat}} \cos\left(\varphi + \frac{\pi}{6}\right) \quad (28)$$

$$t_1 = -t_2 + T_S \left(\frac{1}{2} - \frac{\sqrt{2} V_S \sin\varphi}{V_{bat}}\right) \quad (29)$$

$$t_3 = T_S - t_1 - t_2 \quad (30)$$

Sector 3 and 4 ($\frac{\pi}{3} < \varphi < \frac{4\pi}{3}$)

The switching time equation is:

$$\vec{V}_S T_S = \vec{V}_1 t_1 + \vec{V}_3 t_3 + \vec{V}_4 t_4 \quad (31)$$

The vector decomposition of the above equation along Real and Imaginary axes in Figure 4:

$$T_S = t_1 + t_3 + t_4 \quad (32)$$

$$Real: \quad V_S T_S \cos\varphi = -V_1 t_1 \cos\frac{\pi}{3} + V_3 t_3 \cos\frac{\pi}{3} - V_4 t_4 \cos\frac{\pi}{6} \quad (33)$$

$$Imag: \quad V_S T_S \sin\varphi = -V_1 t_1 \sin\frac{\pi}{3} + V_3 t_3 \sin\frac{\pi}{3} + V_4 t_4 \sin\frac{\pi}{6} \quad (34)$$

3. Simulation Results

The simulation is done by SIMULINK/MATLAB. The inverter is a full-bridge IGBT with extra switches that during the fault tolerant control, one leg (phase C) is connected to the middle point of a capacitor bank by one of the extra switches. The controller has a braking-chopper switch to control the bus voltage. Also it has a closed-loop (PI) speed regulation block. Electrical source is a 600Ah Lead-Acid battery. Its voltage, nominal discharge current and internal resistance is 650V, 600A and 10mΩ respectively. The motor is an induction three-phase squirrel-cage motor and its rated values and parameters are in Table 4.

Table 4 motor rated values and parameters

Power	15KW
Voltage(line-line)	460V
Frequency	60Hz
Speed	1760rpm
Pole pair(p)	2
Rs	0.276Ω
Rr	0.164Ω
Ls	0.0021H
Lr	0.0021H
Lm	0.076H
J	0.1Kg.m^2
f	0.017N.m.s

The system starts and runs normally in six-switch inverter algorithm with no load. It increases and regulates the speed to 1500RPM. The speed is regulated after t=0.75s (Figure 5). At t=1s, 40N.m load is connected to the motor. At t=1.25, the load is increased to full load 70N.m. At t=2s, the fault is occurred and the leg C is faulty (Figure 5). System continues to run by SVM six-switch inverter algorithm. Figures 5 and 7, and Figures 5 and 10 show the stator current and electromagnetic torque are increased with distortion respectively. At t=2.2s, the modified SVM algorithm for four-switch inverter; operating in parallel before fault; is performed and connects the leg C to the middle point of a capacitor bank by send a signal command to the extra switch. Figures 5 and 8, and Figures 5 and 11 show the stator current and electromagnetic torque are reduced respectively and the distortion is reduced. Figure 6 is shown that speed regulation has ripple during t=2s and t=2.2s until the controller algorithm is changed to modified SVM algorithm for four-switch inverter. Bus voltage has ripple during the fault (t=2s to t=2.2s) (Figure 5). After t=2.5s motor speed is increased to 1760RPM by the modified SVM algorithm for four-switch inverter (Figure 5) that Figure 9 is shown that the stator current behavior is reasonable and it is reduced when the speed is regulated.

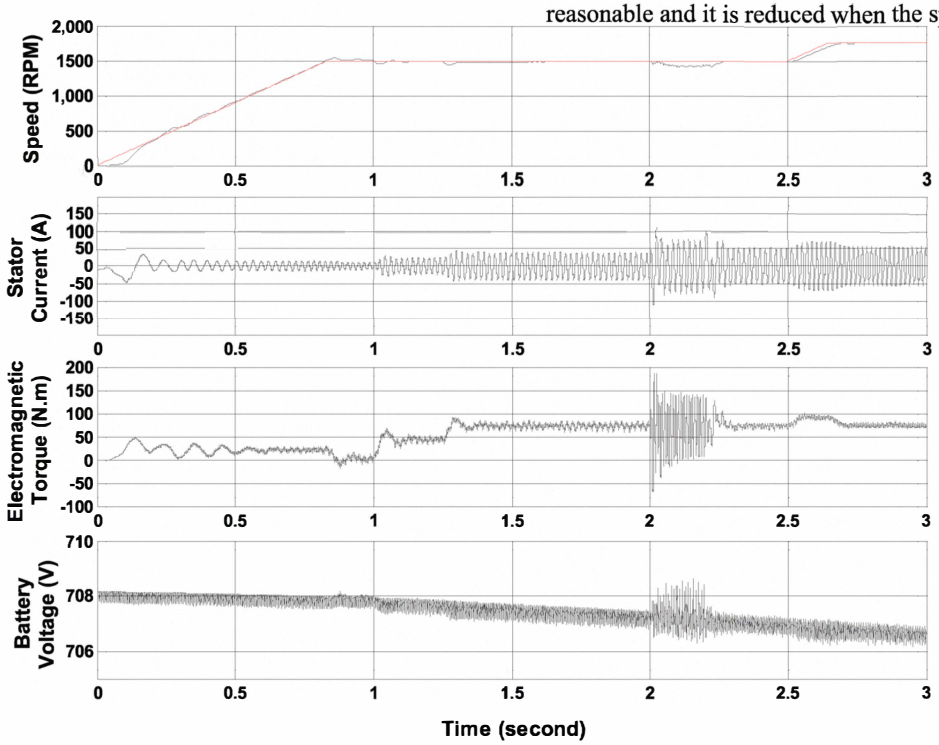

Figure 5. Speed(rpm) & Stator Current(A) & Electromagnetic Torque(N.m) & Bus Voltage(V) vs Time(second)

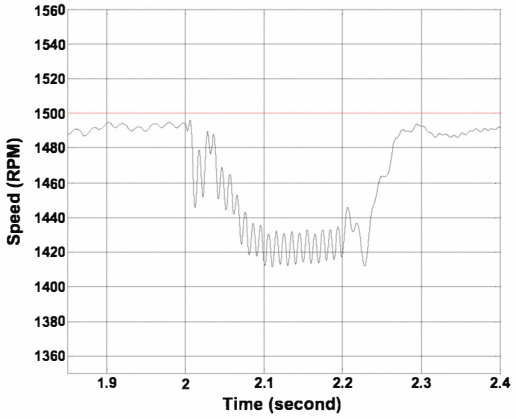

Figure 6. Zoom Speed(rpm) vs Time(second)

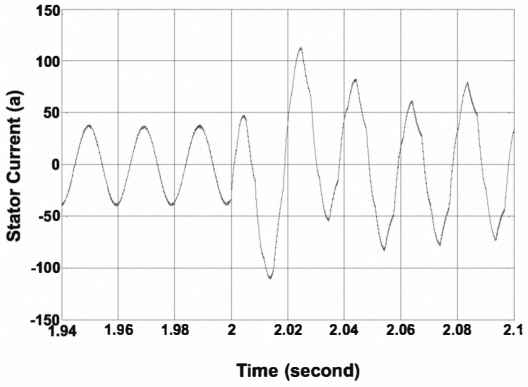

Figure 7. Zoom around t=2s of Stator current(A) vs Time(second)

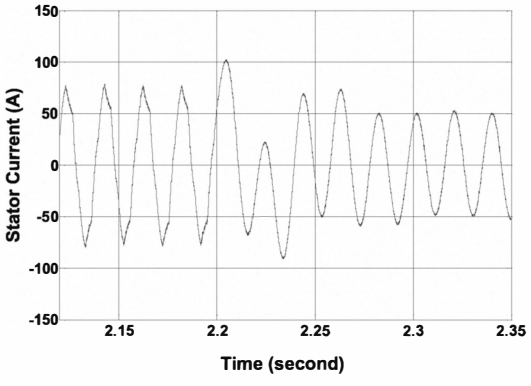

Figure 8. Zoom around t=2.2s of Stator current(A) vs Time(second)

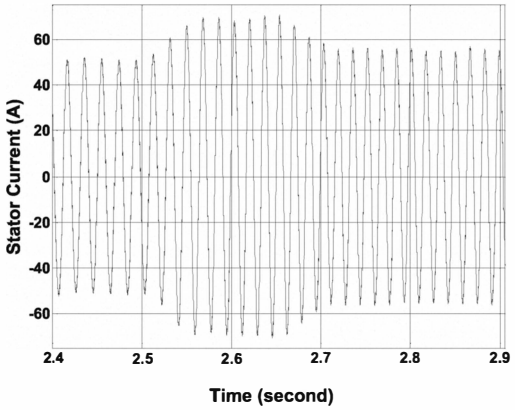

Figure 9. Stator current(A) vs Time(second) when the modified SVM algorithm runs and increases motor speed from 1500RPM to 1760RPM

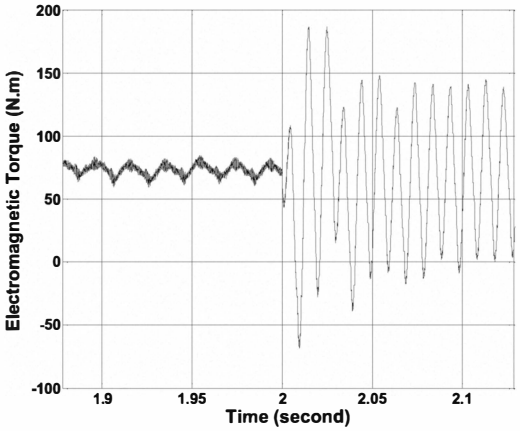

Figure 10. Zoom around t=2s of Electromagnetic Torque(N.m) vs Time(second)

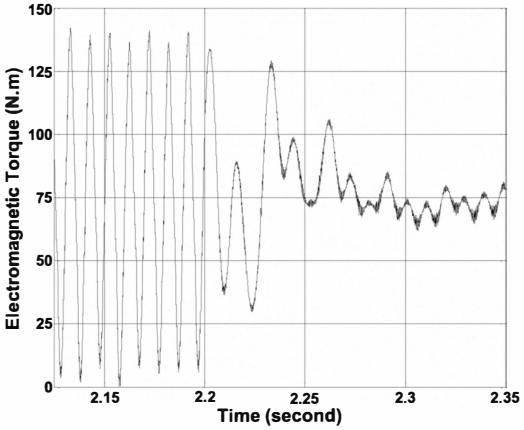

Figure 11. Zoom around t=2.2s of Electromagnetic Torque(N.m) vs Time(second)

4. Conclusion

A low-cost fault tolerant control algorithm based on the SVM technique is presented. The algorithm and the related inverter-motor structure are simple and easy for practical implementation; in fact the algorithm does not require the motor modeling and parameters. The fault-tolerant control includes two main algorithms; one for three-leg and the other for two-leg inverter; operating in parallel. In case a fault occurred on the inverter legs (open- or short-circuit) the algorithm changes-over on the mentioned algorithm.

The proposed control algorithm is verified by using a 15kW/460V/60Hz induction motor simulated with SIMULINK/MATLAB. The results obtain from simulation show stator current, electromagnetic torque and speed regulation behaviors reach desirable states by fault tolerant control. These states are very similar to six-switch inverter algorithm results without fault.

References

[1] C. C. Chan, "The state of the art of electric and hybrid vehicles," *Proc. IEEE, vol. 90, no. 2, pp.247-275, Feb.2002.*

[2] M. E. H. Benbouzid et al., "A loss-minimization DTC scheme for EV induction motors," *in Proc. IEEE VPPC, Chicago, IL, Sep. 2005, pp. 315-321.*

[3] Babak Fahimi, Handbook of automotive power electronics and motor drives, Chapter 26, "Fault tolerant adjustable speed motor drives for automotive applications".

[4] D. Kastha and B. K. Bose, "Investigation of fault modes of voltage-fed inverter system for induction motor drive ," *IEEE Trans. Ind. Applicat.*, vol. 30, pp. 426-433, July 1994.

[5] M. E. H. Benbouzid, "Bibliography on induction motors faults detection and diagnosis," *IEEE Trans. Energy Conversion*, vol. 14, pp. 1065-1074, Dec. 1999.

[6] Brian A. Welchko, Thomas A. Lipo, Thomas M. Jahns, and Steven E. Schulz, "Fault tolerant three-phase AC motor drive topologies: A comparison of features, cost, and limitations," *IEEE Trans. Power Electronics.*, Vol. 19, NO. 4, July 2004.

[7] M. E. H. Benbouzid, D. Diallo, and M. Zeraoulia, "Advanced fault-tolerant control of induction-motor drives for EV/HEV traction applications: from conventional to modern and intelligent control techniques," IEEE Trans. Vehicular Technology., Vol. 56, NO. 2, March 2007.

[8] M. Monfared, H. Rastegar, H. M. Kojabadi, "Overview of modulation techniques for the four-switch converter topology," PECon 08, 1-3 Dec 2008, Johor Baharu, Malaysia.

[9] T. M. Jahns, "Improved reliability in solid-state ac drives by means of multiple independent phase-drive units, " *IEEE Trans. Ind. Applicat.*, vol.IA-16, pp. 321-331, ay/June 1980.

[10] T. H. Liu, J. R. Fu, and T. A. Lipo, "A strategy for improving reliability of field-oriented controlled induction motor drives," *IEEE Trans. Ind. Applicat.*, vol. 29, pp. 910–918, Sept./Oct. 1993.

[11] J. R. Fu and T. A. Lipo, "A strategy to isolate the switching device fault of a current regulated motor drive," in Conf. Rec. *IEEE IAS Annu.Meeting,* vol. 2, 1993, pp. 1015–1020.

[12] R. L. A. Ribero, C. B. Jacobina, E. R. C. da Silva, and A. M. N. Lima, "A fault tolerant induction motor drive system by using a compensation strategy on the PWM-VSI topology," in Conf. Rec. *IEEE Power Electronics Spec. Conf.,* vol. 2, 2001, pp. 1191–1196.

[13] R. L. A. Ribero, C. B. Jacobina, A. M. N. Lima, and E. R. C. da Silva, "A strategy for improving reliability of motor drive systems using a four-leg three-phase converter," in *Conf. Rec. IEEE APEC'01*, vol. 1, 2001, pp.385–391.

Biographies

Hamed Shahsavari Alavije was born in Tehran, Iran, on April 11, 1986. He received B.E.E and M.S.E.E degrees from Shahed University, Tehran, in 2008 and 2011.

His experiences are in analog circuit design, power electronic and motor drive. In 2007, he joined to Electrical Car Team (Rojan) in Amirkabir University of technology, where he worked on electronic circuit and motor control.

His hobbies are reading book, making photoshop image, climbing, swimming and microstrip antenna design.

Mahdi Akhbari received the B.Sc. degree from Ferdowsi University of Mashad, Mashad, Iran, in 1993, the M.Sc. degree from Sharif University of Technology, Tehran, Iran, in 1995, and the Ph.D. degree from the Polytechnic of Grenoble, Grenoble, France in 2000, all with honors in electrical power engineering. Since 2000 he has been with the Department of Electrical Engineering at Shahed University, Tehran, Iran, where he is currently an Assistant professor. Dr. Akhbari's main research interests include modeling, analysis, design, and control of power electronic converters/systems and its application in Power system. In collaboration with industries and consulting engineering companies as technical advisor he has been involved in different applied researches; his experience encompasses conceptual design, detailed engineering and training in power system analysis, industrial power system protection, protection coordination and power quality analysis.